Low complexity modelling and predictive control of a distillation column

B. Huyck [*,**,***] **F. Logist** [**] **J. De Brabanter** [*,***]
J. Van Impe [**] **B. De Moor** [***]

[*] *Department of Industrial Engineering, KaHo Sint Lieven, Gent, Belgium (e-mail: Bart.huyck@esat.kuleuven.be)*
[**] *Department of Chemical Engineering (CIT - BioTeC), K.U.Leuven, Leuven, Belgium*
[***] *Department of Electrical Engineering (ESAT - SCD), K.U.Leuven, Leuven, Belgium*

Abstract: This research project aims at implementing model predictive controllers (MPC) on low level industry standard hardware as Programmable Logic Controllers (PLCs), and validating these controllers on industrial processes. Hereto, a pilot scale distillation column set-up is employed as a test example. The current paper presents the first steps in this direction: (i) the identification of a low complexity model and (ii) the successful validation of a PC based linear MPC controller. More precisely, two MISO transfer function models have been identified and combined into one MIMO model, which has been incorporated into a Matlab model predictive controller implemented in Simulink. In future, the translation of the current control approach to less computationaly powerful hardware (as PLCs) will be explored.

Keywords: System Identification; Linear MIMO; Chemical Industry; Distillation Columns; Automatic Process Control; Model-Based Control

1. INTRODUCTION

In a world where economic and environmental issues become more and more important, efficient control systems have become indispensable. One of these control systems is Model Predictive Control (MPC). This control strategy is widely spread in chemical industry, but other industry branches are less familiar with MPC applications. The need for a model which may be expensive to construct [Mathur et al., 2008] and non standard hardware requirements are disadvantages that slow down the introduction of MPC in these parts of the industry. Since Programmable Logic Controllers (PLCs) with less computational power than PC's are used a lot in industry for control, it is interesting to explore the possibilities and limitations of these devices for MPC. If these devices are suitable and manufacturers can equip their PLCs with an integrated MPC controller, the introduction of MPC will be easier. The weak computer power of PLCs justifies the choice for linear transfer function models in this paper. Moreover, transfer function models are commonly used in industry and most of industrial MPC applications use linear empirical models [Qin and Badgwell, 2003].

As an industrial example, a pilot-scale binary distillation column, is selected. The column is currently controlled by PI controllers, but the goal is to upgrade the control system with a linear MPC running on a PLC. However, before a model based controller can be used on a PLC, an accurate (but simple) process model has to be constructed. Hence, this paper will derive a black-box Multiple Input Multiple Output (MIMO) transfer function model for the column and use this model in a model predictive controller. As a first step towards control on PLC, the model predictive controller will be implemented on PC. Hence, this paper focuses on the identification of the column and model predictive control on PC.

The paper is organized as follows. Section 2 describes the binary distillation column. Section 3 presents the identification procedure covering data collection and preparation, model selection and validation. The resulting model is implemented in an MPC controller in Section 4. Finally, Section 5 summarises the main conclusions.

2. DISTILLATION COLUMN SET-UP

The experimental set-up involves a computer controlled packed distillation column (see Figures 1 and 2). The column is about 6 m high and has an internal diameter of 6 cm. The column works under atmospheric conditions and contains three sections of about 1.5 m with Sulzer CY packing (Sulzer, Winterthur) responsible for the separation. This packing has a contact surface of 700 m^2/m^3 and each meter packing is equivalent to 3 theoretical trays. The feed stream containing a mixture of methanol and isopropanol is fed into the column between the packed sections 2 and 3. The temperature of the feed can be adjusted by an electric heater of maximum 250 W. At the bottom of the column a reboiler is present containing two electric heaters of maximum 3000 W each. In the reboiler, a part of the liquid is vaporised while the rest is extracted as bottom stream. At the column top a total condenser

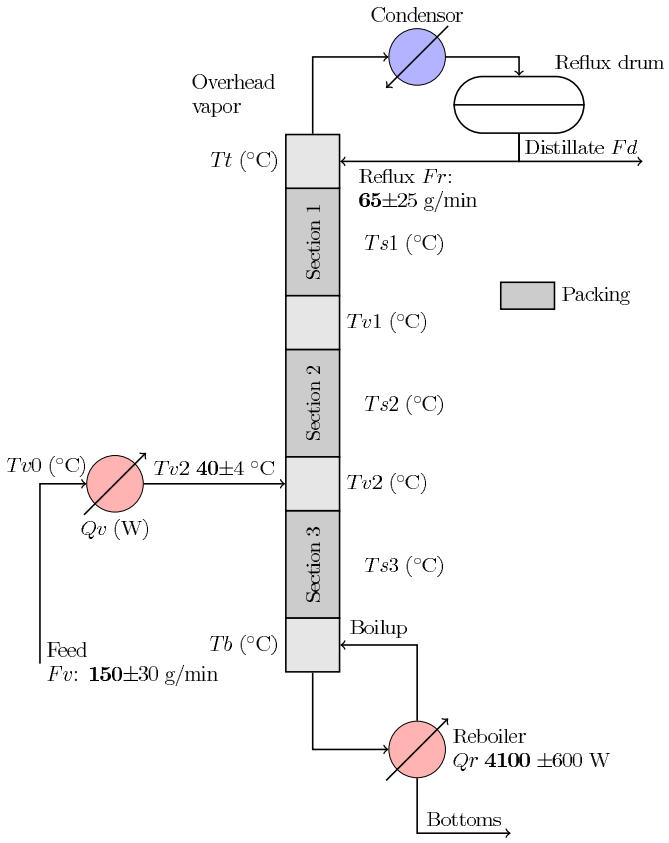

Fig. 1. Diagram of the pilot scale distillation column. Nominal set-points are printed in bold and are followed by the maximum admissible deviations.

allows to condense the entire overhead vapour stream, which is then collected in a reflux drum. A part of the condensed liquid is fed back to the column as reflux, while the remainder leaves the column as the distillate stream.

In this set-up the following four variables can be manipulated: the reboiler duty Qr (W), the feed rate Fv (g/min), the duty of the feed heater Qv (W) and the reflux flow rate Fr (g/min). The distillate flow Fd (g/min) is adjusted to maintain a constant reflux drum level. Measurements are available for the reflux flow rate Fr, the distillate flow rate Fd, the feed flow rate Fv and nine temperatures, i.e., the temperature at the top of the column Tt, the temperatures in the center of every packing section (i.e. $Ts1$, $Ts2$ and $Ts3$, respectively), the temperature $Tv1$ between section 1 and 2, the temperature $Tv2$ between section 2 and 3, the temperature Tb in the reboiler of the column, and the temperatures of the feed before and after heating (i.e. $Tv0$ and $Tv2$, respectively). All temperatures are measured in degrees Celsius. The actuators and sensors are connected to a Compact Fieldpoint (National Instruments, Austin) with a controller interface cFP-2100 and I/O modules cFP-AIO-610, cFP-AIO-610 and cFP-AI-110. A Labview (National Instruments, Austin) program has been developed to control the actuators and to register the variables. There is no online measurement of the concentrations in the distillate and bottom stream, but they can be inferred from the temperatures.

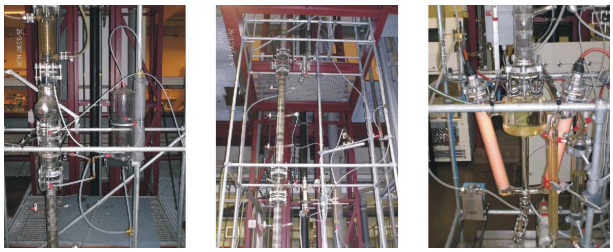

Fig. 2. Pictures of the pilot-scale distillation column: condenser (left), packed section and feed introduction (center), and reboiler (right).

3. MODEL IDENTIFICATION

Devices with limited computer power require a model with limited complexity. Therefore linear process models are chosen. In order to construct the model following steps are performed: (*i*) Experiment, (*ii*) Data preparation, (*iii*) Model selection and Parameter estimation, and (*iv*) Validation. The processing is performed using the Matlab System Identification Toolbox [Ljung, 2009].

3.1 Experiments

In order to generate estimation and validation data for system identification, three experiments are performed. Two of them are build up with Pseudo Random Binary (PRB) signals and one consists of step signals of the different manipulated variables. Before the excitation signals are applied, the column is kept at a constant operating point for two hours to ensure the column is in steady-state. The nominal steady-state values of the different manipulated variables are: a reflux flow rate Fd of 65 g/min, a feed flow rate Fv of 150 g/min, a feed heater duty Qv to maintain a feed temperature $Tv2$ of 40 °C and a reboiler power Qr of 4100 W. These nominal values are known to yield an appropriate operating point for the column. All manipulated variables are controlled by PI controllers except the reboiler power. When the column has reached steady-state, experiments are started.

When the excitation signals are applied, all manipulated variables stay between 2 values. The reflux flow rate Fr varies between 40 and 90 g/min, while the feed flow rate Fv changes between 120 and 180 g/min. The feed heater duty Qv is manipulated to obtain feed temperatures Tv between 38 and 42 °C and the reboiler power Qr switches between 3500 and 4700 W. The distillate flow rate Fr is manipulated such that the content of the reflux drum is kept at 40% of its maximum content. All data are recorded with a sampling period of 100 ms.

The first PRB input signal is constructed in the following way. The reboiler duty Qr is a repeated periodic signal of 6000 s. The clock period, i.e. the minimum time before the signal is allowed to switch, is 300 s. From former experiments [Logist et al., 2009], it is known that the dynamics of the system are faster at the top of the column. Therefore, the clock period of the other inputs is slightly smaller. For the feed flow rate Fv and feed temperature $Tv2$ a clock period of 120 s is taken by a period of length 3720 s and for the reflux flow rate Fr the clock period is 20 s with a period length of 5100 s. These input signals are

$$\begin{bmatrix} Tt \\ Tb \end{bmatrix} = \begin{bmatrix} \frac{-2.26}{(1+2565s)(1+135s)} & \frac{0.53}{1+735s} & \frac{3.74}{(1+1803s)(1+78s)} & \frac{-3.45}{(1+2698s)(1+72s)}e^{-53.3s} \\ \frac{-2.13}{(1+1098s)}e^{-77.9s} & \frac{0.89}{1+1551s} & \frac{5.37}{2980s+1}e^{-37.1s} & \frac{-2.42}{(1270s+1)(545s+1)} \end{bmatrix} \begin{bmatrix} \text{Fv} \\ \text{Qv} \\ \text{Qr} \\ \text{Fr} \end{bmatrix} \quad (1)$$

combined into one experiment with a time span of 25000 seconds. The second experiment is slightly slower. The periodic signal has a length of 8000 s for all manipulated variables and the clock period for Qr, Fv, $Tv2$ and Fr is 500 s, 120 s, 120 s and 60 s respectively. The step input signal excites only one variable at the time. All manipulated variables are switched from there nominal to the lowest, the highest and back to the nominal value as written above. A sufficient amount of time has been waited before each switch to ensure the set-up reaches steady-state.

3.2 Model in- and outputs

The considered outputs of the system are two temperatures along the column, i.e., the top temperature Tt and the bottom temperature Tb. An overview of the different in- and outputs is depicted in Figure 3.

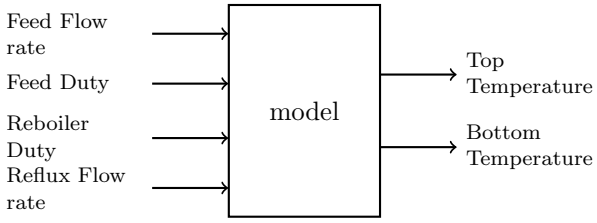

Fig. 3. Overview of the in- and outputs of the column model.

3.3 Data preparation

The sampling period of the three recorded datasets is reduced to 10 s. Therefore every 10 s a sample is taken from the original record data without averaging or filtering. Before identification, an identification and a validation dataset has to be created. These datasets are created the following way. Both PRB datasets are split up into 2 sections: the first 2/3 and the remainder 1/3. Together with de complete step dataset, these 5 datasets are combined randomly into an identification and a validation part which are used in the identification process.

3.4 Model selection and parameter estimation

The aim is to construct a linear MIMO black-box model for the distillation column. This model will be created from a set of MISO submodels. Based on first principles insights, distillation columns consist of low order subsystems. Therefore linear, low-order, continuous-time transfer functions are fitted to the data. A first order model (Eq. 2), a damped second order model (Eq. 3) and an undamped second order model (Eq. 4), all with time delay are estimated.

$$G(s) = \frac{K_p}{1+T_{p1}s}e^{T_d s} \quad (2)$$

$$G(s) = \frac{K_p}{(1+T_{p1}s)(1+T_{p2}s)}e^{T_d s} \quad (3)$$

$$G(s) = \frac{K_p}{1+2\xi T_w s+(T_w s)^2}e^{T_d s} \quad (4)$$

For all combinations of identification and validation datasets, these models types are estimated and compared to each other. The model type for each of the four inputs is choisen the same. Before validation, these models are compared to each other based on their estimated parameter set. Models with unrealistic parameters such as time constants longer than the experiment time and unrealistic high gains were removed. The resulting models are listed based on the fit value.

3.5 Validation

As model validation, the prediction of the dataset is compared with the measured data based on a Fit measure (Eq. 5) and the Mean Squared Error (MSE). The Fit measure is defined as:

$$\text{Fit} = 100\% \left(1 - \frac{|\hat{y}(t) - y(t)|}{|y(t) - \bar{y}(t)|}\right) \quad (5)$$

where $\hat{y}(t)$ is the predicted output, $y(t)$ the measured output, $\bar{y}(t)$ the mean of the measured output and $|.|$ is the 1-norm of the vector in between. A Fit value of 100% means that the prediction is the same as the measure output. If the predicted value is the mean value, the result is 0%. The MSE is the sum of squared errors between the measured and estimated temperature, divided by the number of samples. The square root of the MSE gives an idea of the mean absolute error between the predicted and measured signal. The lower this value, the better.

3.6 Results

This section describes the results for different types of linear, low-order, continuous-time transfer functions

Model identification With the different sets of validation and estimation data, first and second order models were estimated as described in section 3.4. The resulting models are ranked based on their Fit value. For the resulting best model, second order sub models with time constants differing more than a factor 1000, are reduced to a first order model and re-estimated with the same estimation dataset. At the same time, time delays smaller than 10^{-6} are removed. The resulting models for the top and bottom temperature are combined into one MIMO transfer function model given in Eq. (1) with time constants and delays in seconds.

The time constants of this model are in a range from 100 until 3000 s. From physical insight of the system, one can presume all subsystems have a time delay. This is not the case, but several second order models without time delay appear. The second order pole masks in these cases the time delay. If re-estimation based on a first order transfer function with time delay instead of a second order system resulted in a worse Fit value, the second order subsystem has been preserved.

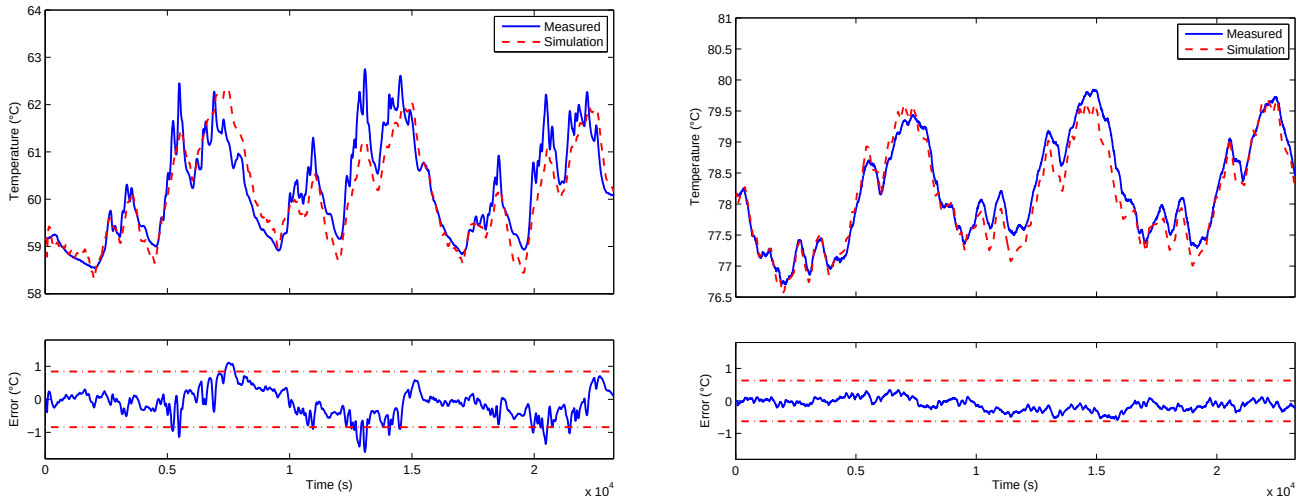

(a) Top temperature (b) Bottom temperature

Fig. 4. Validation of the different temperatures. As validation dataset, the second experiment with PRB excitation signals is taken. Each figure depicts the simulation above and the error between the measured and simulated signal below. The dash-dot line indicates the 20% error band.

Model validation The final models for the top and bottom temperature are estimated on the dataset with step data and a combination of step data and the last one third of the first PRB dataset respectively. Figure 4(a) and Figure 4(b) depict the validation plot for the top and bottom temperature respectively. As the second PRB dataset is used for none of the model estimations, this dataset is used for validation for both models. Both figures also contain a plot with the error between the measured and the simulated temperature.

As can be seen on Figure 4(a), the simulation follows the trend of the measured temperature well, although some peaks are not captured. Especially, sharp peaks and fast variations are not covered by the model. This is also presented by the error plot were one can see that the absolute temperature error leaves the 20% error band. This corresponds to 0.84 °C as the top temperature is excited over a range of 4.2°C. The fast varying peaks are believed not to disturb the control action of the controller due to the long time constants of the model, although they cause the Fit value to be as low as 56% and the MSE value to be as high as 0.2 (Table 1). The square root of the MSE value is 0.44 °C, the mean error during the whole experiment.

For the bottom temperature, the error stays within the 20% error band which corresponds to an error of 0.6°C. Figure 4(b) depict that these time peaks are covered very well. The Fit value is 74% and MSE value is as low as 0.04 (Table 1). The corresponding mean error is 0.2 °C. These values demonstrate that this model is of high quality and it will be illustrated that this model performs very well for control.

3.7 Conclusion

The model identification results in a MIMO model composed from two MISO linear continuous-time transfer function models. The MISO model describing the bottom temperature captures the dynamics of the system very well and the error stays below 20%. The top temperature model has difficulties capturing the fast varying temperature so the error at some peaks is more than 20%. Nevertheless, as the error is fast varying, the model describes the main trend. Both models are combined and the resulting MIMO model will be employed for model predictive control purpose in the next section.

Table 1. Fit and MSE values for the top and bottom temperature.

	Fit (%)	MSE
Top temperature	56	0.20
Bottom temperature	74	0.04

4. MODEL PREDICTIVE CONTROL

In this section, a model predictive controller is developed based on the model identified in the previous section. To assess the quality of control, the Relative Gain Array will (RGA) be computed. Simulation and finaly implementation of the controller on the pilot-scale distillation column prove the insight given by the RGA.

4.1 Model analysis

Relative Gain Arrray One of the possibilities to investigate the coupling between the input and output is the Relative Gain Array (RGA) [Shinskey, 1988, Glad and Ljung, 2000, Mc Avoy et al., 2002]. This is a measure of the influence of a controlled variable, relative to other controlled variables. Elements close to one are the preferred control variables for that output. Elements close to zero are of less influence for the corresponding output. Input-output connections with negative elements indicate an inverse reaction and should be avoided if possible.

The RGA From Eq. (1) is:

	Fv	Qv	Qr	Fr
Tt	0.3688	-0.0411	-1.0201	1.6923
Tb	-0.1792	0.0783	1.9547	-0.8537

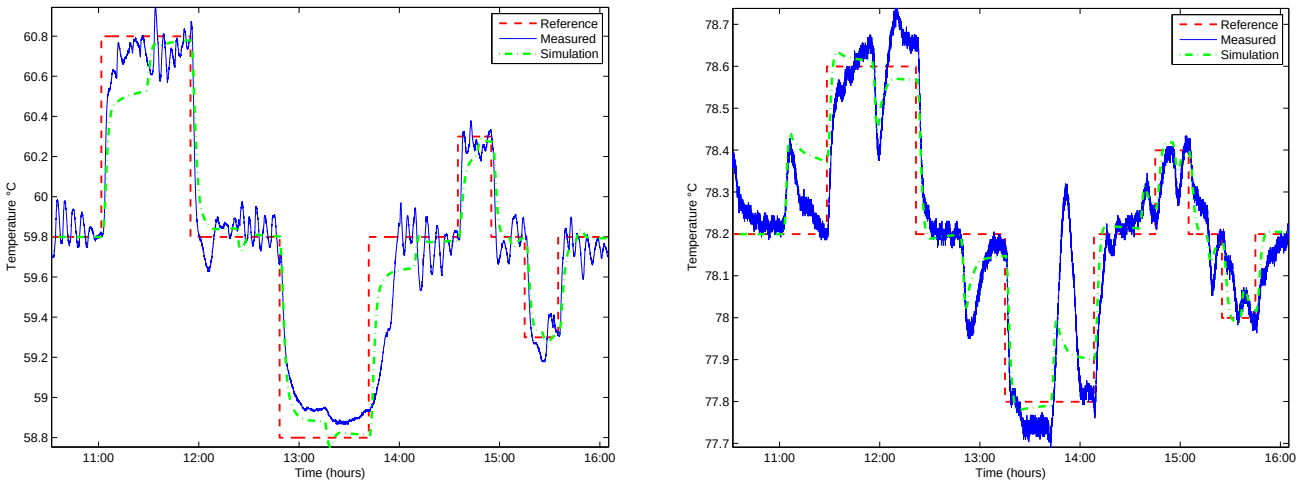

(a) Controled top temperature (Tt)

(b) Controled reboiler temperature (Tb)

Fig. 5. Simulation and measurements of an experiment on the pilot scale distillation column for the outputs with the proposed settings of the model predictive controller.

This matrix indicates a strong influence of the reflux flow rate Fr on the top temperature Tt and an inverse gain for the reboiler power Qr. The bottom temperature Tb is strong determined by the reboiler power and in an inverse way by the reflux flow rate Fr. As stated above, negative elements must be avoided. Hence, when adapting the top temperature, only the reflux has to be manipulated and the reboiler power kept constant. This is exactly the opposite as for the adaptation of the bottom temperature, which demonstrate that control is difficult. Manipulating one of the two temperatures will always disturb the other.

Both the feed flow rate and feed heating duty have a low impact as there corresponding values in the RGA are close to zero. The preferred inputs to manipulate both temperatures are Qr and Fr. Fv and Qv are of less influence and are only useful for small corrections.

4.2 Model preparation

The identified model is a continuous time model. Model predictive controllers used in practice are discrete controllers. Therefore the model is converted to a discrete state space model with minimal realisation. The sampling time is chosen to be 60 seconds. The resulting state space model is a 15th order model.

4.3 Controller design

The controller from the Matlab model predictive control toolbox [Bemporad et al., 2009] is used to control the pilot-scale distillation column. A prediction and control horizon of 100 and 30 time steps is taken respectively. In order to keep the power consumption of the complete system approximately constant, the penalty for the reboiler and feed heating power is twice the penalty of the flow rates. The penalty of the input moves is the same for all control variables.

The values of the different input signals are constrained. The reboiler power is bound between 3000 and 5000 W and the reflux flow rate is allowed to move in a range between 45 and 95 g/min. The constraints for the feed flow rate are 100 and 200 g/min and the feed duty varies between 0 and 225 W. The outputs are considered of equal importance, so the penalty on the deviation of the desired value is equal.

4.4 Simulation and test-run of the controller

With the designed controller, simulations are performed. Figure 5(a) and 5(b) illustrates a simulation of the top and the bottom temperature respectively. As can be seen, not all desired temperatures are reached. In all cases where the set-point differs from the steady state value, one output reaches the desired values while the other moves away from its set-point. Due to the settings of the controller, the set-points of the last manipulated variable supersedes the former set-points and the temperatures move to another value.

On the pilot-scale set-up the same reference trajectory is applied to both temperatures. As the column is a nonlinear system controlled by a linear controller, deviations from the simulation can be expected. For the top temperature, one can see that the real system reacts faster when the temperature is moving up, but slower when the temperature decreases. For the small steps of 0.5 °C at the end, this behaviour is less clear and one can take the view that the system is faster than the simulation. During the experiment, a low frequent disturbance signal is present at the top temperature. This is caused by the PI level controller of the reflux drum. The regulating valve has a large hysteresis which need a redesign of the current PI controller, which is considered future work.

The reboiler temperature Tb (Figure 5(b)) is excited with a smaller amplitude. The measured signal seems more noisy than the signal of the top temperature, but this is caused by the resolution of the sensor. Some large peaks catch the eye. These are caused by a set-point change of the top temperature. From the RGA, one can see that if the top temperature has to be changed, the reboiler power has to be adapted too. This causes the bottom temperature to change. For the top temperature, the reflux flow rate

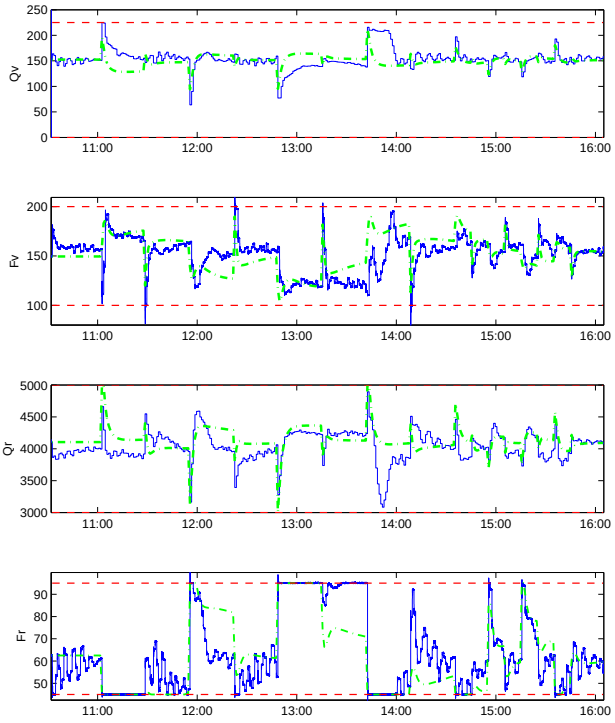

Fig. 6. Simulation and measurements of an experiment on the pilot-scale distillation column for the inputs. The solid lines are the measurements, the dotted lines the simulation and the dashed lines are the constraints of the different inputs.

is able to correct for a reboiler duty change. The feed flow rate and feed duty have small values in the RGA. This means their influence is limited. Hence, they are not powerful enough to correct for a bottom temperature change if the reflux flow rate is unavailable, causing the large peaks.

When comparing both figures, it seems impossible to get both temperatures at the desired value at the same time except when at least one temperature is at the steady state value. This demonstrates that in the future, depending on what the purpose is, a relative degree of importance of the temperatures will have to be made. Although the quality of the top temperature model is less than the quality of the bottom model, this seems no problem for the controller.

In Figure 6, the inputs and the simulated inputs of the system are depicted. Of course the measured and simulated inputs are different as the controller has to deal with unmeasured disturbances. Despite these disturbances, the simulated and measured inputs resemble each other. The small peaks that cross the constraints for the flow rates are caused by the overshoot of the different PI controllers. The reflux flow Fr touches the constraints quite a long time, certainly between 13h and 14h. This obliges the other three inputs to change in order to follow the set-point changes. This causes the high peak just before 14h. This is also an indication that set-point changes for the top temperature further away from the steady state temperature will be hard to get. Both flow rates, Fv and Fr violate the constraints at some points, but this is due to the PI settings of the corresponding controllers. Tuning The PI parameters of these controllers to a step answer without overshoot, will solve the constraint violations in the future.

5. CONCLUSION

In this paper, a begin has been made for implementing model predictive controllers (MPC) on low level industry standard hardware such as Programmable Logic Controllers (PLCs). Therefore, a low complexity multiple input, multiple output model is created for a pilot-scale distillation column, composed from two multiple input, single output identified transfer function models. The model has been successfully validated and is employed as a base for a model predictive controller. Currently the Model predictive control is PC based and has proven to be successful. Further research will now focus on the translation of model predictive control algorithms to low level industry standard hardware.

REFERENCES

A. Bemporad, M. Morari, and N. L. Ricker. *Model Predictive Control Toolbox 3 Users Guide*. The MathWorks, Inc, Natick, 2009.

T. Glad and L. Ljung. *Control Theory: Multivariable and Nonlinear Methods*. Taylor and Francis, London, 2000.

L. Ljung. *System Identification Toolbox Users Guide*. The MathWorks, Inc, Natick, 2009.

F. Logist, B. Huyck, M. Fabre, M. Verwerft, B. Pluymers, J. De Brabanter, B. De Moor, and J. Van Impe. Identification and control of a pilot scale binary distillation column. In *Proc. ECC 09*, pages 4659–4664, 2009.

U. Mathur, R. D. Rounding, D. R. Webb, and R. J. Conroy. Use model-predictive control to improve distillation operations. *Chem. Eng. Prog.*, 104:35–41, 2008.

T. Mc Avoy, Y. Arkun, R. Chen, D. Robinson, and P.D. Schnelle. A new approach to defining a dynamic relative gain. *Con. Eng. Prac*, 11:907–914, 2002.

S. J. Qin and T. A. Badgwell. A survey of industrial model predictive control technology. *Con. Eng. Prac.*, 11:733–764, 2003.

F. G. Shinskey. *Process Control Systems, Application, Design, and Tuning*. McGraw-Hill Publishing Company, New York, third edition, 1988.

ACKNOWLEDGEMENTS

BDM is a full professor at the Katholieke Universiteit Leuven, Belgium. Research supported by: Research Council KUL: GOA AMBioRICS, GOA MaNet, CoE EF/05/006 Optimization in Engineering(OPTEC), IOF-SCORES4CHEM, IOF HBKP/06/002; OT/03/30; OT/09/025; KP/09/005, several PhD/postdoc & fellow grants; Flemish Government: FWO: PhD/postdoc grants, projects G.0452.04 (new quantum algorithms), G.0499.04 (Statistics), G.0211.05 (Nonlinear), G.0226.06 (cooperative systems and optimization), G.0321.06 (Tensors), G.0302.07 (SVM/Kernel), G.0320.08 (convex MPC), G.0558.08 (Robust MHE), G.0557.08 (Glycemia2), G.0588.09 (Brain-machine) research communities (ICCoS, ANMMM, MLDM); G.0377.09 (Mechatronics MPC). IWT: PhD Grants, McKnow-E, Eureka-Flite+, SBO LeCoPro, SBO Climaqs, POM Belgian Federal Science Policy Office: IUAP P6/04 (DYSCO, Dynamical systems, control and optimization, 2007-2011) ; EU: ERNSI; FP7-HD-MPC (INFSO-ICT-223854), COST intelliCIS, EMBOCOM.

J. Van Impe holds the chair Safety Engineering sponsored by the Belgian chemistry and life sciences federation essenscia.